PHYSICAL REVIEW B VOLUME 39, NUMBER 9 15 MARCH 1989-II

Alkali-metal oxides. II. Unoccupied and excited states

E. Bertel, N. Memmel, W. Jacob, and V. Dose
Max-Planck-Institut für Plasmaphysik–EURATOM Association, Boltzmannstrasse 2, D-8046 Garching bei München, Federal Republic of Germany

F. P. Netzer, G. Rosina, G. Rangelov,* and G. Astl
Institut für Physikalische Chemie, Universität Innsbruck, A-6020 Innsbruck, Austria

N. Rösch, P. Knappe, and B. I. Dunlap†
Lehrstuhl für Theoretische Chemie, Technische Universität, Müchen, D-8046 Garching bei München, Federal Republic of Germany

H. Saalfeld
Fachbereich Physik, Universität Osnabrück, Barabarastrasse 7, Postfach 4469, D-4500 Osnabrück, Federal Republic of Germany
(Received 28 March 1988; revised manuscript received 7 October 1988)

The unoccupied electronic levels of NaO_2 and KO_2 have been probed by inverse photoemission. In addition, excitation spectra of various core and valence levels have been recorded with use of x-ray absorption spectroscopy and electron-energy-loss spectroscopy. Results from a linear combination of Gaussian-type orbitals $X\alpha$ (LCGTO-$X\alpha$) model cluster study and photoemission data previously reported give a coherent and detailed description of ground- and excited-state properties of the alkali-metal superoxides. This description includes molecular and crystal-field effects, excitonic properties of the excited states, and electron-hole correlation energies as well as transition-matrix-element effects.

I. INTRODUCTION

In the preceding paper we have reported photoemission data obtained from thin films of alkali-metal superoxides.[1] It has been shown that the valence photoemission can be explained entirely in terms of the O_2^- molecular-orbital structure modified by crystal-field effects. In the present paper we report on the unoccupied-level structure of these compounds as revealed in soft-x-ray photoabsorption (XAS), electron-energy-loss spectroscopy (ELS) and inverse photoemission (IPE). The data are also compared to linear combination of Gaussian-type orbitals $X\alpha$ (LCGTO-$X\alpha$) calculations carried out for NaO_2 model clusters. Using all the information obtained by the various spectroscopic methods and by the theoretical approach we are able to give a comprehensive assignment of initial and final states. As a result of this effort a more detailed understanding of excitonic core-level excitations in ionic compounds emerges. Transition-matrix-element effects are elucidated by comparing the excitation spectra of different core and valence levels. In addition quantitative estimates on electron-hole correlation energies in these insulating compounds are given.

The paper is organized as follows. Section II is devoted to the technical details of both the experimental setup and the computational procedure. Section III first reports the results of the model cluster calculation. Second, the results of the core excitation spectroscopy on NaO_2 and KO_2 are presented and discussed. In Sec. III C we report on the valence ELS and the IPE spectra of the two alkali oxides. Section III D gives a summary of the information obtained from the different spectroscopic methods. Relative cross sections of the various excitations are discussed qualitatively and correlation energies are derived. In Sec. IV the electronic level structure of the alkali superoxides as established in the present study is briefly summarized.

II. EXPERIMENTAL AND COMPUTATIONAL DETAILS

A. Experiment

The preparation of the alkali-metal superoxide films has been carried out *in situ* under UHV conditions. The detailed procedures of film preparation have been described in the preceding paper.[1] XAS spectra have been recorded at the toroidal grating monochromator TGM-2 of the synchrotron radiation laboratory BESSY in Berlin (Berliner Elecktronenspeicherring-Gesellschaft für Synchrotronstrahlung) by monitoring the secondary electron yield at fixed kinetic energy while sweeping the photon energy through the near threshold region of various core levels [constant–final-state spectroscopy (CFS)]. The spectra have been corrected by the monochromator transmission as measured with photodiodes and via the total photocurrent from the gold mirror following the monochromator stage. The two correction methods yielded similar results in the energy regions of interest, thereby indicating only minor second-order radiation effects. The XAS and IPE spectra have been obtained from the corrected data by subtraction of a parabolic

background. The energy analysis of the secondary electrons has been performed in a modified VG Instruments ADES 400 Spectrometer equipped with a spherical sector analyzer.

The ELS spectra have been obtained in a different UHV chamber featuring a concentric hemispherical analyzer (CHA) (Leybold Heraeus LH 10) and an electron gun 45° off the analyzer axis. The overall resolution of this setup was 500 meV as measured on the full width at half maximum (FWHM) of the elastically reflected beam. Special care has been taken to avoid beam damage effects. Comparison of spectra obtained from oxide films which had accumulated increasing beam exposures showed that electron-beam induced changes in the spectra were negligible under the conditions applied to record the spectra shown in the present study. However, we were not able to record core-level ELS spectra at primary energies $E_p \gtrsim 600$ eV without introducing significant radiation damage. Supplementary measurements of the beam damage by electron-stimulated ion desorption (ESD) showed a strong increase of the ion yield beyond the oxygen 1s core-level threshold at ~ 530 eV in agreement with the indirect observations made on the ELS spectra. At lower primary energies the ion yield consisted mainly of O^+ ions whereas at high primary energies also Na^+ could be detected. As a consequence of these results primary energies have been limited to be below 500 eV for recording ELS spectra.

The IPE spectra have been measured in a third UHV system featuring a low-energy, high-current gun and an I_2 Geiger-Müller counter with CaF_2 window[2] resulting in a 0.7 eV overall resolution. The spectra have been obtained under normal electron incidence using a photon collection angle of 37° off normal.

B. Computational procedure

In the subsequent interpretation of the electronic structure of alkali oxides we will draw extensively on the analogy between NaO_2 and NaCl which becomes evident when one views the crystal structure of the former compound as being obtained by replacing Cl ions by O_2 groups. Local excitonic features of NaCl in an energy range similar to the present study have recently been reassigned on the basis of linear combinations of Gaussian-type orbital (LCGTO) $X\alpha$ model cluster investigations.[3] It therefore seemed profitable to supplement the spectroscopic information for NaO_2 by results from corresponding model calculations.

The model cluster used in the present study was constructed by surrounding a Na ion by its six nearest-neighbor O_2 groups in the crystal. Interatomic distances were taken from experiment:[4] 1.33 Å for the bond length of O_2^-, 2.74 Å for the distance from the center of the O_2 groups towards the central Na ion. The resulting average Na—O bond distance is 2.82 Å, the shortest nonbonding O-O distance 3.06 Å (for our idealized geometry given below). There is no obvious choice for the orientation of the O_2 ligands in the model cluster. Depending on temperature, NaO_2 exists in at least three phases.[4] Under the prevailing experimental conditions NaO_2 crystallizes in a cubic pyrite structure with essentially rotationally disordered O_2 groups.[4] In the pyrite structure the axes of the oxygen anions are aligned diagonally with respect to the cubic lattice, resulting in point-group symmetry S_6 of a $Na^+(O_2^-)_6$ model cluster. Because of the above-mentioned disordering of the ligands it seems justified to save computational effort by using a model cluster with a somewhat higher point-group symmetry, D_{3d}. This symmetry may be derived from the S_6 structure by rotating the O_2^- groups about their respective centers by an angle of 35.2°.

To simulate the crystal environment this cluster was embedded in a lattice of 86 point charges which includes all sites of a NaCl-type lattice up to the forth shell of nearest neighbors. The point charges were adjusted so that the resulting potential at the central Na site reproduces the value of the Madelung potential of such a crystal under the constraint of charge neutrality of the cluster.[3]

The electronic structure of this model cluster was calculated using the $X\alpha$ variant of the local density functional method as implemented in the muffin-tin–free LCGTO technique.[5–7] This method has been shown to provide a satisfactory description of a wide variety of metal complexes[8–10] including a recent study of local excitons in NaCl.[3] Three basis sets are employed in a LCGTO-$X\alpha$ calculation, one to expand the molecular orbitals and two to fit the charge distribution and the exchange potential, respectively. For the Na ion these basis sets were taken from the NaCl study[3] for which a $(12s,9p,7d)$ molecular-orbital (MO) basis had been constructed, which is flexible enough to describe final states of type 3s, 3p, and 3d in the field of a 2p hole. The basis sets for oxygen were chosen according to standard procedures.[5,11] A $(9s,5p)$ MO basis[12] was augmented by d polarization functions with an exponent of 1.15 (Ref. 13) and contracted to $(6s/4p/1d)$. The quality of this basis was checked by calculating the molecules O_2 and O_2^-. For the ground state a bond length of 1.22 Å for O_2 and of 1.38 Å for O_2^- was obtained, the vibrational frequency being 1556 cm^{-1} for O_2 and 1129 cm^{-1} for O_2^-. The agreement with the corresponding experimental values[14] (O_2: 1.21 Å, 1580 cm^{-1}; O_2^-: 1.35 Å, 1140 cm^{-1}) is very satisfactory in both cases, supporting the view that the bases are rich enough to describe the changes in the electronic structure of the O_2 molecule brought about by the addition of one electron.

All excitations for the NaO_2 system have been obtained from separate spin-polarized calculations for the ground state and for the various excited states (ΔSCF method). To guarantee well-behaved self-consistent-field (SCF) convergence a high-spin configuration was chosen in all cases, i.e., in the 12 molecular orbitals arising from linear combinations of O_2^- orbitals six holes were placed with like spin. Excited states were derived from this configuration by transferring one electron from the Na-type 2p level into a formerly unoccupied level of interest. The transition energies were essentially independent of the involved spin orientation (differences below 0.2 eV). The values presented below are therefore given for an ad-

ditional hole with minority spin and a final state of majority spin with the exception of a transition into the ligand π_g-type orbitals, which can be achieved in our model with the minority spin-orbital manifold only (this type of excitation provided well-behaved SCF convergence for all cases of interest).

III. RESULTS AND DISCUSSION

A. Model cluster calculation

Before presenting any experimental or theoretical results on NaO_2 it is useful to recall some concepts that have been employed successfully in the interpretation of Na^+ L_{23} spectra of sodium halides. While being also typically ionic crystals, the simpler structure of the latter compounds facilitates working out the salient features of their soft-x-ray spectra.[15] We shall restrict the following discussion to NaCl since the lattice constant of this compound [5.64 Å (Ref. 16)] is rather similar to that of NaO_2 [5.49 Å (Ref. 4)].

Åberg and Dehmer[17,18] first explained the discrete structures in the soft-x-ray spectra of NaCl in terms of highly localized excitons. These features below or slightly above the threshold for photoconduction [36.0 eV (Refs. 19, 20)] are associated with quasiatomic "inner well" final states of the alkali ion localized inside the first shell of anions. The different peaks represent transitions from the occupied Na $2p$ level into the unoccupied Na $3s$ and $3d$ levels, the latter being split by the octahedral ligand field.

Compared to the corresponding excitation energies of a free Na ion one observes lower values due to the destabilizing effect of the Madelung potential on the electronic levels. Since this energy shift is larger for tightly bound core levels their distance from more diffuse valence levels is effectively reduced. For the same reason one finds the difference between the Na $3s$- and the Na $3d$-type final states reduced in a crystal environment. However, the postulated level inversion of the $3p$-type and the $3d$-type final states[17,18] was not supported by the model cluster study[3] which placed this transition energetically close to the lower one of the two $3d$-type final states. The experimental excitation energy for the transition into the Na $3p$-type final state remained uncertain for NaCl since it is symmetry forbidden. A further, quite unexpected result of the cluster calculation was the level ordering $e_g < t_{2g}$ for the two Na $3d$-type final states, which is caused by the rather diffuse character of the $3d$-type orbitals leading to a dominant π-type metal ligand interaction.[3]

The $X\alpha$ valence orbital energies of the model cluster $Na^+(O_2^-)_6$ are displayed in Fig. 1. Only spin-averaged energies are shown for the sake of clarity. Above the filled manifold of O_2^- π_u levels between -8.0 eV and -10.0 eV one finds the half-filled manifold of the O_2^- π_g levels between -3.0 and -4.5 eV. This ground-state distribution of the O_2 valence orbitals deviates somewhat from the relative energy positions measured in UPS. This may in part reflect the difficulty of correctly representing deep valence orbitals of O_2 in the LCGTO-$X\alpha$ approach.[21] On the other hand, final-state effects in UPS

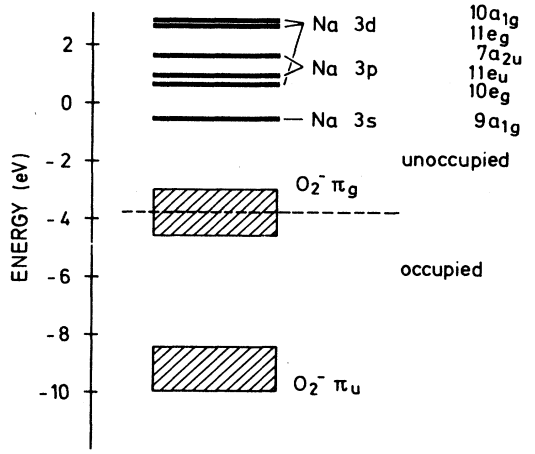

FIG. 1. The LCGTO-$X\alpha$ valence orbital energies for the model cluster $Na^+(O_2^-)_6$. The main orbital components of the levels are given together with the symmetry assignment for each level in D_{3d} point-group symmetry.

are important for the rather localized O_2 valence orbitals as will be shown further below. Also shown in Fig. 1 are the empty Na $3l$-derived levels ($l=s,p,d$) above -0.5 eV. From the cluster study on $NaCl_6$ it is known that their ordering roughly parallels that of the corresponding atomic excitation energies. The lowest-level $9a_{1g}$ is of Na $3s$ type. Due to the reduced symmetry the Na $3d$-derived levels are split into $10e_g$ and $11e_g$. From the energetic spacing of these $3d$-derived levels together with the remaining $10a_{1g}$ orbital one predicts (despite the reduced symmetry) essentially the same pattern as found for the NaCl cluster. In Table I the calculated excitation energies for the transitions out of the Na $2p$ level are displayed and compared to experimental peak energies (see below). One notices a ligand field splitting of the Na $3d$-derived excitation energies of about 2.0 eV quite similar to the value found for NaCl. The splitting of the $3p$-type levels is somewhat smaller (0.7 eV). From the theoretical results of Table I one also expects metal-to-ligand charge-transfer excitations (Na $2p \rightarrow O_2^-$ π_g) in the energy range 30–40 eV.

There are a number of ways in which the electronic

TABLE I. Comparison of experimental (ELS, XAS) and theoretical (LCGTO-$X\alpha$) excitation energies for NaO_2 (in eV).

Transition					
From	To	Theory	ELS[a]		XAS
$2p$	π_g	30.60	30.6	(A)	
$2p$	$3s$ ($9a_{1g}$)	32.70	31.7	(B)	31.6
$2p$	$3d$ ($10e_g$)	33.88		(C)	
$2p$	$3p$ ($11e_u$)	34.15	33.6		33.7
$2p$	$3p$ ($7a_{2u}$)	34.87		(D)	
$2p$	$3d$ ($11e_g$)	35.91	36.6	(E)	36.3
$2p$	$3d$ ($10a_{1g}$)	35.96			

[a]Labeling of the ELS peaks as in Fig. 2.

structure of the alkali superoxides differs significantly from that of NaCl. In NaO_2 the lowest empty electronic levels are not formed by the Na $3l$ and nl conduction-band states but by O_2^- empty molecular orbitals (MO's). The lowest unoccupied level in the O_2^- molecule derives from the $\pi_g(2p)$ antibonding orbital, which is partially occupied as shown in Fig. 1.

Photoemission results indicate that in the alkali superoxides this level retains its MO character just as, for example, in condensed oxygen.[1] Therefore we conclude that it is not much involved in the conduction-band formation but remains rather localized. The next higher unoccupied O_2^- MO is the strongly antibonding $\sigma_u(2p)$ level which may contribute to the higher conduction-band states. As the Na core-level excitations probe mainly states with large amplitudes at the sodium site, the final states with the largest oscillator strength will contain mainly Na $3l$ contributions. As already pointed out, these states are conduction-band states. However, the presence of the core hole at the cation site introduces considerable excitonic effects. This statement is substantiated by a comparison of UPS and IPE with ELS results given below, which demonstrate that the electron-hole interaction in the Na core-level excitations amounts to about 4 eV. Accordingly the final state of the excited core electron cannot be considered as a Bloch state but requires a localized description. Henrich and coworkers[22] have demonstrated that for Mg core-level excitations in MgO the atomic final state description worked well despite some conceptual difficulties. The localization introduced by the considerable electron-hole interaction and the sodium site specificity of the Na core-level excitations result in a close analogy to the localized exciton picture of core-level excitations in NaCl, notwithstanding considerable differences in the ground-state electronic structure.

B. Core-level spectra of NaO_2 and KO_2

Figures 2 and 3 show core-level excitation spectra of NaO_2. In Fig. 2 the near-edge region of the Na $2p$ level is examined by XAS and ELS. The core-level excitations observed in XAS obey strictly the dipole selection rules, whereas in ELS dipole-forbidden transitions may be excited with increasing probability as the primary electron energy drops towards the threshold.[23] In the ELS spectra of Fig. 2 the threshold at about 30 eV is followed by the three peaks A, B and C,D at 30.6, 31.7, and 33.6 eV excitation energy, respectively. The peak C,D at 33.6 eV is composed of two different structures, as will become obvious below, and therefore has been doubly labeled. A pronounced minimum is observed at 35.4 eV in all spectra of Fig. 2 and from this minimum additional features E and F extend to about 42 eV excitation energy. The XAS spectrum has been cut off at about 37 eV because at this energy direct emission from the Na $2p$ level starts to enter into the fixed kinetic energy window. The Na $2p$ photoemission binding energy has been measured relative to the substrate Fermi level to be $E_{PE}(\text{Na } 2p) = 31.8$ eV in Ref. 1.

In the XAS spectrum peak A is missing and therefore

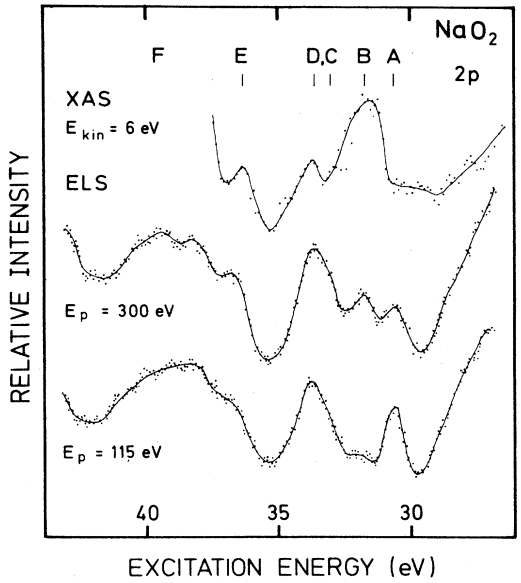

FIG. 2. Na $2p$ core-level excitation spectra of NaO_2. The topmost curve is the x-ray absorption spectrum obtained by recording the secondary electron yield at 6 eV kinetic energy. The two lower curves represent ELS spectra recorded at different primary energies E_p.

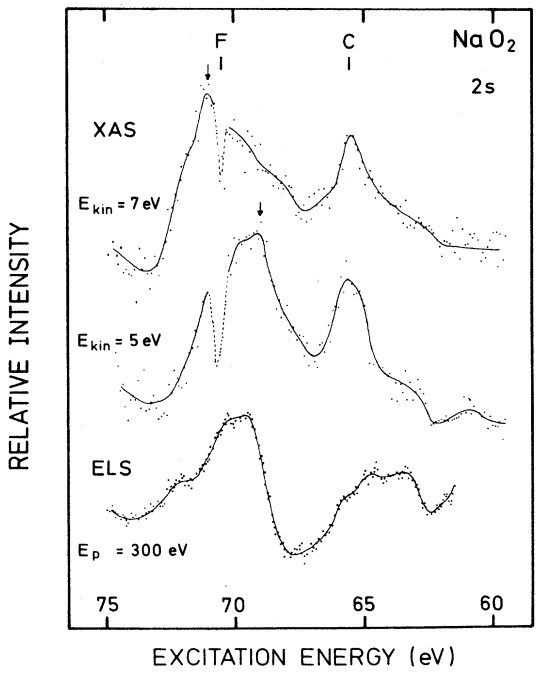

FIG. 3. Na $2s$ core-level excitation spectra of NaO_2. The two upper curves are x-ray absorption spectra measured by recording the secondary electron yield at two different fixed kinetic energies E_{kin}. The arrows mark the Na $2s$ direct photoemission feature. The lower curve is an ELS spectrum obtained at a primary energy $E_p = 300$ eV.

can be identified as a nondipole transition. The dipole-forbidden character of peak A is also borne out by its strong increase in relative intensity as the primary energy in ELS is lowered. Peak B behaves in just the opposite way and is therefore readily associated with a dipole transition. As the structure C,D shows an intermediate behavior it is tentatively interpreted as a superposition of a dipole and a nondipole transition.

In Fig. 3 XAS and ELS spectra of the Na $2s$ threshold region are shown. The threshold occurs at 62.5 eV. The Na $2s$ binding energy has not been measured in paper I,[1] but the two XAS spectra recorded at $E_{\text{kin}}=7$ eV and $E_{\text{kin}}=5$ eV which are presented in Fig. 3 show the Na $2s$ direct emission feature appearing at 71 and 69 eV photon energy, respectively (arrows). From this a Na $2s$ binding energy $E_{\text{PE}}=64.0$ eV is derived. The sharp dip at 70.5 eV photon energy in the XAS spectra is apparently an artifact caused by spurious Al $L_{2,3}$ absorption in the beam line.

Similar to the Na $2p$ ELS spectra the Na $2s$ ELS spectrum shows a triply peaked structure between the threshold and a pronounced minimum about 5.5 eV above threshold. The intensity distribution, however, is rather different. The only dipole-allowed transition within the energy range of 5 eV above threshold appears in the XAS spectra at 65.5 eV, i.e., 3.0 eV above the onset. This is at the same energy above threshold where the feature C,D had appeared in the $2p$ ELS spectra and it reveals the composite character of this excitation in ELS.

In order to obtain an assignment of the near-edge structures shown in Figs. 2 and 3 we consider at first the XAS data because there dipole selection rules are strictly applicable. In the Na $2s$ XAS spectrum of Fig. 3 the lowest energy peak is expected to arise from a Na $2s\rightarrow 3p$ excitation. The corresponding final state will remain triply degenerate (t_{1u}) for octahedral symmetry. Further symmetry reduction by the axial O_2^- molecule causes a splitting of the t_{1u} level into e_u and a_{2u}, but this may be considered as a second-order effect causing only a peak broadening in the XAS spectrum. Consequently we assign peak C in the XAS spectra of Fig. 3 to an excitonic Na $2s\rightarrow 3p$ excitation.

In the Na $2p$ core-level spectra this excitation is dipole forbidden. The dipole-allowed $2p\rightarrow 3s$ and $2p\rightarrow 3d$ transitions, however, should produce three different final states because the octahedral component of the crystal field will split the d-derived levels into e_g and t_{2g} states, again under the assumption that lower-symmetry components cause only minor effects (see also Fig. 2). Accordingly we associate the first and dominating XAS peak B in Fig. 2 with the Na $3s$-derived final state, whereas the peaks D and E are assigned to the crystal-field split e_g and t_{2g} states. As the ELS spectra reflect a very similar final-state distribution for both the $2s$ and the $2p$ excited states we conclude that the dipole-forbidden $2p\rightarrow 3p$ excitation peak should occur at about 3.2 eV above threshold. This is just the position C where the primary energy dependence of the ELS spectra in Fig. 2 suggested a dipole-forbidden contribution to appear.

The proposed level ordering with peak B corresponding to the $3s$ final state, peak C bearing $3p$ character and finally peaks D and E relating to the crystal-field–split d levels is at variance with the assignments given by Åberg and Dehmer[17,18] for the Na $2p$ absorption spectrum in NaCl, because it does not invoke a pronounced p-d level inversion. The present assignment, however, is also supported by the calculations described in the preceding paragraph. The calculated excitation energies do not exhibit the same uniform trend as in the case of NaCl where they were found to be systematically too low by an amount of about 1 eV. The error with respect to the experimental values can be correlated with the spatial extension of the final state. The tighter the final orbital the larger is the difference from the experimental value. However, this deviation never exceeds 1 eV and is comparable to the errors in the excitation energies of the free sodium ion (about 0.6 eV) whether calculated with the LCGTO-$X\alpha$ or with a numerical $X\alpha$ method.[3]

The results for the transition energies support the physical concept underlying the cluster model and the model itself. The structure between 31.0 and 37.0 eV (peaks B to E in Fig. 2) may be attributed to strongly localized excitonic transitions. The final states can be characterized as sodium $3s$, $3p$, and $3d$ type and may therefore be described quite appropriately as quasiatomic "inner well" states similar to the sodium-chloride crystal. Peak B can be assigned to the $2p\rightarrow 3s$ transition. Also straightforward is the association of the high-energy feature of the spectra where peak E is due to the transitions $2p\rightarrow 3d$ (a_{1g},e_g).

The explanation of peaks C and D which appear at similar energy is more tedious because they have to represent three transitions $2p\rightarrow 3d$ (e_g) (optically allowed) and $2p\rightarrow 3p$ (a_{2u},e_u) (optically forbidden) if our model is to be considered adequate. The presence of features in both $2s$ and $2p$ excited spectra and the primary energy dependence of feature C,D in the $2p$ ELS confirm the composite nature of the structure C,D and support the proposed model approach.

In contrast to NaCl (O_h) the lower point-group symmetry of the NaO_2 compound (S_6, or D_{3d} in our model), results in a splitting of the sodium $3p$ type final state and the removal of the threefold degeneracy of the octahedral t_{2g} set arising from $3d$-type orbitals. Inspecting the $3d$-type final state we found three levels ($10e_g$, $11e_g$, and $10a_{1g}$). Because of the small energy difference between the $11e_g$ and $10a_{1g}$ level (0.05 eV), which contrasts to their distance to the $10e_g$ level (about 2.05 eV), we conclude that these levels belong to the t_{2g} state in the octahedral case. We observe therefore the same ordering in the Na $3d$-derived final state as in the case of the NaCl with $e_g<t_{2g}$. The overall d-level splitting is calculated to be of the order of 2 eV, which is somewhat smaller than the 2.7 eV obtained from the spectra in Fig. 2. As pointed out by Rösch *et al.*[3] for NaCl, the actual splitting results from the crystal field and the strong π interaction of the Na $3d$ (t_{2g}) with the O_2^- π_g orbitals. In view of this intricate balance the agreement between experiment and theory is quite satisfying.

The broad, structured peak F which appears in all spectra of Figs. 2 and 3 is most likely associated with

higher *ns*-, *np*-, and *nd*-derived conduction-band states. The different shape of this structure in the 2*p* and 2*s* excitation spectra indicates that it does not merely reflect the density of states but, despite being degenerate with the conduction band, bears nevertheless excitonic character. This parallels the conclusions drawn by Pantelides[19,20] for the XAS spectra of alkali halides.

In contrast to NaCl an additional peak below the $2p \rightarrow 3s$ transition is found by 30.6 eV in the ELS (peak *A* in Fig. 3) whose intensity shows a strong dependence on the primary energy indicating an optically not allowed transition. The present calculations explain these peaks as charge-transfer excitations into unoccupied ligand π_g levels (see Fig. 1).

Let us now contrast the K 3*p* XAS spectra of KO_2 to those of NaO_2. Figure 4 shows a series of constant final-state spectra obtained from KO_2 at kinetic energies ranging from 4.3 to 7.5 eV and photon energies $13 \leq h\nu \leq 25$ eV corresponding to the threshold region of the K 3*p* core-level excitation. The K 3*p* binding energy in KO_2 is $E_B = 17.3$ eV (Ref. 1) and the highest-binding-energy valence photoemission feature $\sigma_g(^1\Pi_g)$ appears at 9.3 eV binding energy.[1] Both levels will give a direct emission contribution to the spectra presented in Fig. 4. This contribution, however, is easily separated from the true photoabsorption peaks by its final-state energy dependence. In the CFS spectra of Fig. 4 the direct emission features are marked by arrows whereas the position of true photoabsorption peaks is indicated by bars. Estimating the position of the threshold at 15.4 eV from the bottom spectrum ($E_{kin} = 7.5$ eV) the first maximum appears 0.8 eV above threshold at 16.2 eV, the second at 18.2 eV, and the third at 20.7 eV.

The dipole-allowed transitions in this case are the $3p \rightarrow 4s$ and the $3p \rightarrow 3d$ (e_g, t_{2g}) excitations. The 3*d* wave function in K is much more localized than in Na, which has at least three important consequences in this context. Firstly, the Madelung potential on the positive lattice site lifts the more localized 3*d* state in energy relative to the less localized K 4*s* and 4*p* states. Therefore it remains well above the 4*s* final state in contrast to the corresponding excitation energies in the free K ion.[24] A similar effect is observed in KCl.[25] Consequently we assign the XAS peak at 16.2 eV in KO_2 to the $3p \rightarrow 4s$ transition and the peaks at 18.2 and 20.7 eV to the crystal-field-split $3p \rightarrow 3d$ (t_{2g}, e_g) transitions. As a second consequence of the strong K 3*d* localization the $p \rightarrow d$ transition is similar in intensity to the $p \rightarrow s$ transition, in contrast to what is observed in NaO_2. Finally, the reduced size of the K 3*d* state results in a considerably smaller π interaction of the t_{2g} with the O_2^- valence orbitals. Therefore the crystal-field-split levels should appear in their "natural" order $t_{2g} < e_g$ in KO_2. Although this conclusion has not yet been confirmed by cluster calculations, it is supported by experimental data presented below.

C. Valence electron-energy-loss and inverse-photoemission spectroscopy

Figure 5 presents a comparison between core-level ELS, valence ELS, and IPE spectra obtained from NaO_2. The spectra have been aligned at their thresholds with

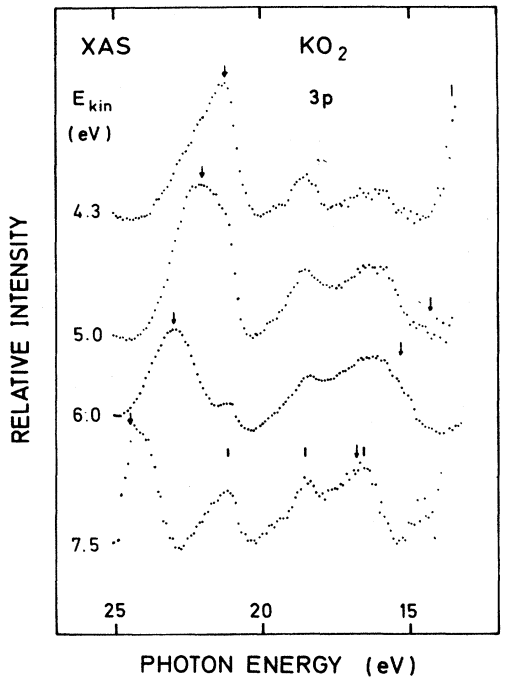

FIG. 4. X-ray absorption spectra of K 3*p* threshold region recorded at different secondary electron energies. Arrows mark the K 3*p* direct photoemission feature at 20–25 eV and the O_2^- $\sigma_g(^1\Pi_g)$ emission at 13–18 eV.

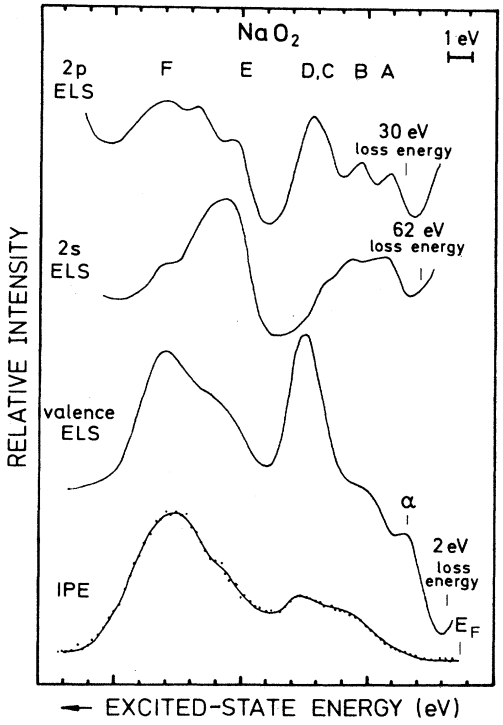

FIG. 5. Comparison of core-excitation, valence-excitation, and inverse photoemission spectra of NaO_2. For details see Sec. III B.

the exception of the valence ELS. The valence ELS has been shifted so as to align the characteristic minimum about 6 eV above threshold and feature E,F with the other spectra. A similar comparison is presented in Fig. 6 for KO_2. On the abscissa an energy scale is given for determination of relative transition energies. Absolute transition energies can be obtained by using the reference energies given for each spectrum in Figs. 5 and 6. The transition energies have been listed in Table II.

The lowest valence ELS peak labeled α occurs in both compounds, NaO_2 and KO_2, at 3.4 eV. Both oxides exhibit a light yellow color[4] indicating the onset of the optical absorption to occur in the blue region of the visible spectrum. We therefore conclude that the 3.4-eV energy loss can be associated with the lowest dipole-allowed transition in the alkali superoxides, which is the π_u-π_g transition on the O_2^- ion. It is superposed on the threshold of the higher valence excitations for which only alkali-derived final states are available. Because of the required wave-function overlap the π_g antibonding orbital is the only initial state participating with a measurable oscillator strength in these excitations. Given a single initial state, the valence excitations in NaO_2 can be assigned to the Na 3s-derived final state (5 eV loss), the Na 3p- and 3d- (e_g) related states (7.8 eV loss), and the t_{2g}-derived manifold at a loss energy of $\sim$11 eV. The structure at 13 eV corresponds to excitation into higher conduction-band states possibly also involving O_2^- $\sigma_u(2p)$ final-state character. This assignment of the valence excitations is supported by the similarity with the Na 2p ELS, which exhibits essentially the same final-state structure and is therefore shown for comparison in Fig. 5.

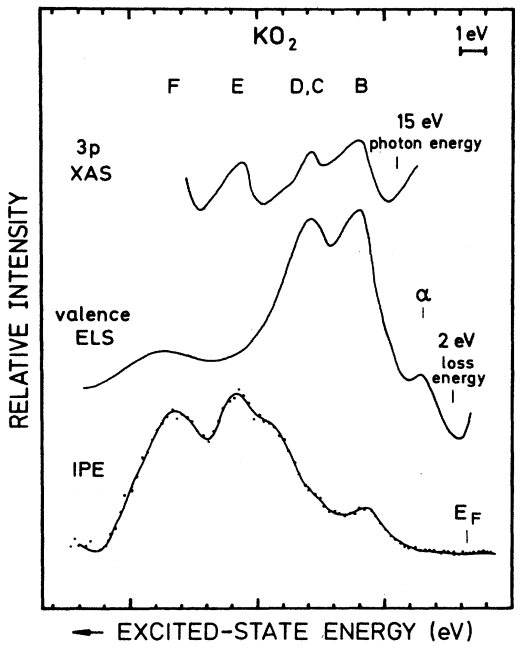

FIG. 6. Comparison of core excitation, valence excitation and inverse photoemission spectra of KO_2. For details see Sec. III B.

TABLE II. Transition energies (eV) in XAS, valence ELS, and IPE.

	Threshold	B	C	D	E	
			2p (3p) XAS			
NaO_2	29.2	31.6	33.7		36.3	
KO_2	15.4	16.2	18.2		20.7	
	α	B	C	D	E	F
			Valence ELS			
NaO_2	3.4	5	7.8		10.8	13
KO_2	3.4	6	7.8		(10)	13
	Threshold	B	C	D	E	F
			IPE			
NaO_2	1	4	6.3		9.4	11.5
KO_2	1	4	(6.2)	7.5	9.3	11.5

The valence ELS of KO_2 presented in Fig. 6 is rather different from the valence ELS of NaO_2. In KO_2 the alkali 3d-derived final states are much more localized on the K site. Consequently the O_2^- $\pi_g \rightarrow$K 3d excitation appears only with negligible intensity in the KO_2 valence ELS and the two pronounced peaks at 6 and 7.8 eV have to be associated with the K 4s- and 4p-related final states.

The different spatial extension of the 3d wave function in NaO_2 and KO_2, respectively, is also reflected in the IPE spectra shown in Figs. 5 and 6. The most pronounced difference between the two spectra is the appearance of a dominating double peak structure at $E-E_F=7.5$ eV and $\sim$9 eV in KO_2, whereas in NaO_2 only minor features are observable in this energy range. Hence the doublet obviously originates from transitions into the K 3d (t_{2g}) and K 3d (e_g) crystal-field-split states. The feature occurring in the NaO_2 and KO_2 IPE at $\sim$4 eV above E_F is assigned to the Na 3s- (K 4s) derived level. In NaO_2 the unresolved 3d (e_g) and 3p states appear in the IPE spectrum at 6.3 eV, the 3d (t_{2g}) level as a weak shoulder at $\sim$9.4 eV above E_F. In KO_2 the 4p-derived structure is obscured by the much stronger 3d doublet. In both IPE spectra a weak threshold is detectable at 1 eV above E_F that is probably associated with the unoccupied part of the O_2^- π_g orbital. Photoemission (PE) from this orbital appears at a binding energy of 4.2 eV (2.4 eV) for NaO_2 (KO_2), respectively.[1] The energy difference between PE and IPE final states is apparently due to incomplete screening of these final states, viz., the self-energy of the π_g hole in photoemission and the correlation energy of the extra π_g electron in the IPE final state. A discussion of the different final-state effects in these complementary spectroscopies is given by Smith and Woodruff.[26] As the larger K^+ ions are more polarizable the screening in KO_2 will be better than in NaO_2 and results therefore in a smaller difference between PE and IPE final states.

Figures 5 and 6 demonstrate that all the spectroscopies applied sample the same final-state distribution. The character of the final states is readily deduced from di-

pole selection rules applicable in the core-level spectra and from the characteristically different behavior of the $3d$-derived states in the IPE and valence ELS spectra of NaO_2 and KO_2.

There remains yet to be discussed an apparent discrepancy in the crystal-field splitting of the empty $3d$ states in NaO_2 and KO_2. In KO_2 this crystal-field splitting amounts to 1.9 eV in the IPE spectrum and 2.5 eV in the K $3p$ core-level XAS. In NaO_2 the $3d$-derived states are less well defined in the IPE spectrum but a splitting of about 3 eV may be estimated. In the Na $2p$ XAS (Fig. 2) this splitting amounts to only 2.6 eV. Thus the magnitude of the crystal-field splitting shows the opposite trend in the two oxides as one proceeds from the more extended negatively charged final state of IPE to the more contracted neutral core-hole excited final state of XAS. A possible reason for this peculiar behavior is discussed by Rösch *et al.*[3] who found an inversion of the t_{2g}, e_g level ordering for NaCl and NaO_2. The level inversion is caused by the large antibonding π interaction of the Na t_{2g} wave functions with O_2^- valence orbitals. In addition, the σ antibonding interaction of the e_g orbitals with the ligand orbitals is reduced for the rather diffuse Na $3d$ wave function. Thus the large spatial extension of the Na $3d$ wave function gives rise to the rather unusual situation of the t_{2g} levels being 3 eV higher in energy than the e_g states. The slight contraction of the $3d$ wave function in the presence of a $2p$ core hole causes a reduction of this "inverse" splitting in the Na XAS to 2.6 eV. As one proceeds in the Periodic Table from Na to K the $3d$ wave function "collapses" and the normal level ordering $t_{2g} < e_g$ is likely to be restored. An increase of the crystal-field splitting as the wave function is further contracted by the $2p$ core hole in XAS could then result as a consequence of a further reduction of the π antibonding t_{2g}–O $2p$ interaction. This effect is presently under theoretical investigation.

D. Correlation energies

In this section we discuss the transition energies observed by the various spectroscopic techniques presented in Figs. 5 and 6 and summarized in Table II. In all the spectra shown the final states are distributed over a similar energy range *regardless of the initial state.* As a consequence, the observed features can be made to coincide by a *rigid shift* of the spectra. In order to arrive at a more quantitative picture we define an effective electron-hole interaction energy $U_{eh}(i;f)$ in the following way:[27,28]

$$E(f \leftarrow i) = E_{PE}(i) + E_{IPE}(f) - U_{eh}(i;f) ,$$

where $E(f \leftarrow i)$ is the excitation energy in XAS or ELS from the initial state i to the final state f, $E_{PE}(i)$ is the photoemission binding energy of the initial state, and $E_{IPE}(f)$ the inverse-photoemission final-state energy, both defined with respect to the substrate Fermi level. Using the Na $2p$ binding energy $E_{PE}(2p) = 31.8$ eV reported in paper I (Ref. 1)[1] and the peak assignments derived from the comparison in Fig. 5, an electron-hole interaction $U_{eh}(2p;3s,3p,3d) \approx 4$ eV is obtained for NaO_2. From Fig. 3 a Na $2s$ binding energy $E_{PE}(2s) = 64.0$ eV was derived. This binding energy yields $U_{eh}(2s;3p) \approx 4$ eV as for the $2p$ excitation.

In order to determine U_{eh} for the valence ELS we need to know the initial states. Peak α has been attributed to the O_2^- π_u initial state. The binding energy of this feature is $E_{PE}(\pi_u) = 7.3$ eV in paper I.[1] Using $E_{IPE}(\pi_g) = 1.5$ eV, $U_{eh}(\pi_u;\pi_g) \approx 5.5$ eV is obtained for NaO_2. The initial state for the higher valence energy losses is most likely the O_2^- π_g orbital. The corresponding electron-hole interaction is $U_{eh}(\pi_g;3d) = 2.6$ eV.

For KO_2 the following estimates may be derived, based on the data of part I (Ref. 1) and Figs. 4 and 6: $U_{eh}(3p;4s) = 4.8$ eV, $U_{eh}(3p;3d) \approx 6$ eV. This latter value is considerably larger than $U_{eh}(2p;3d)$ in NaO_2 and is characteristic of the large $3p$-$3d$ intrashell interaction in the $3d$ transition metals. From the valence ELS $U_{eh}(\pi_u;\pi_g) = 3.6$ eV and $U_{eh}(\pi_g;4s,4p) = 0.6$ eV are obtained.

The electron-hole correlation energies derived above are in reasonable agreement with orbital overlap considerations and may therefore be taken as an independent confirmation of the present final-state assignment. Nevertheless it is surprising that, for instance in the Na $2p$ ELS spectrum of NaO_2, the structure F shows the same separation from the Na $3(s,p,d)$-derived states as in the IPE spectrum. This indicates a similar electron-hole interaction for both $2p$ excitations into the lower excitonic states as well as the higher conduction-band-derived states, and confirms the conclusion that the electron-hole correlation suffices to introduce a considerable localization even of high-lying conduction-band states. A similar conclusion seems to apply for the valence excitations in NaO_2 despite the considerably lower value of $U_{eh} = 2.6$ eV. In the valence excitation region of KO_2, however, excitations to higher conduction-band states are nearly absent, which is consistent with the small U_{eh} (< 1 eV) found in this case.

It should also be noted that in NaO_2 as well as KO_2 core-level excitation spectra a pronounced dip is observed about 3.7 and 3.0 eV, respectively, above the XPS threshold. A comparison with the IPE spectra in Figs. 5 and 6 shows that this second onset can be identified with the bottom of the conduction band. A similar interpretation has been proposed by Pantelides for related structures in alkali-halide core-level excitation spectra.[19,20]

IV. CONCLUSIONS

The electronic structure of alkali superoxides has been investigated by UPS (Ref. 1) and XAS using synchrotron radiation, by core-level and valence ELS and by IPE. The measurements have been carried out on NaO_2 and KO_2, the latter being representative of the isostructural superoxides of the heavier alkali metals. In addition LCGTO-$X\alpha$ model cluster calculations have been performed in order to evaluate and supplement the information provided by the experiments. The theoretical calculations were based on the local excitonic picture which had been brought forward by Åberg and Dehmer.[17,18]

Using the LCGTO-$X\alpha$ formalism this picture has been refined and corrected for NaCl (Ref. 3) and is finally applied to the more complex compound NaO_2 in the present study. The result of this combined theoretical and experimental effort can be summarized by the following conclusions.

(i) The occupied valence orbitals have almost exclusively the character of O_2^- molecular orbitals. The solid-state environment results mainly in crystal-field induced binding energy shifts leaving these orbitals rather undisturbed otherwise.

(ii) The lowest empty levels are derived from O_2^- π_g orbitals and are also localized on the oxygen sites. The bottom of the conduction band appears at about 1.5 eV above the empty π_g states. The conduction band is formed predominantly from Na-derived wave functions. The $\sigma_u(2p)$ antibonding O_2 orbital seems to contribute only at rather high energy to conduction-band states, i.e., about 6–8 eV above the bottom of the conduction band.

(iii) Core-level excitations, and in NaO_2 valence level excitations, result in excitonic final states. The Na 3*s*, 4*p*, and 3*d* (e_g) and the K 4*s*, 4*p*, and 3*d* (t_{2g}) derived excitonic states fall below the bottom of the conduction band. However, excited states at higher energy which are degenerate with the conduction band are also quite localized as indicated by considerable electron-hole correlation energies. Thus the localized exciton picture holds also for the alkali superoxides and allows a consistent interpretation of the various excitation spectra.

(iv) The differences in the electronic level structure of NaO_2 and KO_2 result mainly from crystal-field effects causing different binding energies of the occupied levels and from the different degree of localization of the unoccupied 3*d*-derived states in Na and K. The latter effect is reflected in dramatically different cross sections for excitations involving 3*d*-derived final states in the two compounds.

(v) LCGTO-$X\alpha$ model cluster calculations yield excitation energies which differ by less than 1 eV from the corresponding experimentally determined energies. Similar to NaCl the calculations indicate an "anomalous" level ordering in NaO_2. This level ordering results from the details of the π and σ interaction between the Na 3*d*–derived states and the O_2^- valence orbitals, which are not appropriately accounted for in simple ligand-field models.

ACKNOWLEDGMENTS

This work has been supported in part by the Austrian Fonds zur Förderung der wissenschaftlichen Forschung, by the Deutsche Forschungsgemeinschaft through Sonderforschungsbereich 128, by the Fonds der Chemischen Industrie and by the Bund der Freunde der Technischen Universität München. Critical reading of the manuscript by J. A. D. Matthew is gratefully acknowledged.

*Permanent address: Institute of General and Inorganic Chemistry, Bulgarian Academy of Sciences, BG-1040 Sofia, Bulgaria.

†Permanent address: Theoretical Chemistry Section (Code 6119), Naval Research Laboratory, Washington, D.C. 20375-5000.

[1]E. Bertel, F. P. Netzer, G. Rosina, and H. Saalfeld, preceding paper, Phys. Rev. B **39**, 6082 (1989).

[2]V. Dose, in *Lectures on Surface Science,* edited by G. R. Castro and M. Cardona (Springer, Berlin, 1987), p. 181.

[3]N. Rösch, P. Knappe, B. I. Dunlap, E. Bertel, and F. P. Netzer, J. Phys. C **21**, 3423 (1988).

[4]N. G. Vannerberg, Prog. Inorg. Chem. **4**, 125 (1962).

[5]B. I. Dunlap, J. W. D. Connolly, and J. R. Sabin, J. Chem. Phys. **71**, 3396 (1979); **71**, 4993 (1979).

[6]B. I. Dunlap, J. Phys. Chem. **90**, 5524 (1986).

[7]J. W. Mintmire and B. I. Dunlap, Phys. Rev. A **25**, 88 (1982).

[8]H. Jörg and N. Rösch, Chem. Phys. Lett. **120**, 359 (1985).

[9]N. Rösch and H. Jörg, J. Chem. Phys. **84**, 5967 (1986); N. Rösch, H. Jörg, and B. I. Dunlap, in *Quantum Chemistry: The Challenge of Transition Metals and Coordination Chemistry,* Vol. 176 of *NATO Advanced Study Institute Series C,* edited by A. Veilland (Reidel, Dordrecht, 1986), p. 179; N. Rösch, P. Knappe, P. Sandl, A. Görling, and B. I. Dunlap, in *The Challenge of d and f Electrons,* edited by D. R. Salahub and M. C. Zerner (ACS, Washington, in press).

[10]N. Rösch, M. Kotzian, H. Jörg, H. Schröder, B. Rager, and S. Metev, J. Am. Chem. Soc. **108**, 4238 (1986); N. Rösch, H. Jörg, and M. Kotzian, J. Chem. Phys. **86**, 4038 (1987).

[11]H. Jörg, N. Rösch, J. R. Sabin, and B. I. Dunlap, Chem. Phys. Lett. **114**, 529 (1985).

[12]F. B. van Duijneveldt, IBM Research Report RJ 945, 1971 (unpublished).

[13]*Gaussian Basis Sets for Molecular Calculations,* edited by S. Huzinaga (Elsevier, Amsterdam, 1984).

[14]K. P. Huber and G. Herzberg, *Constants of Diatomic Molecules* (Van Nostrand, Princeton, 1979).

[15]S. Nakai, T. Ishii, and T. Sagawa, J. Phys. Soc. Jpn. **30**, 428 (1971).

[16]N. W. Ashcroft and N. D. Mermin, *Solid State Physics* (Saunders, Philadelphia, 1976).

[17]T. Åberg and J. L. Dehmer, J. Phys. C **6**, 1450 (1973).

[18]T. Åberg and J. L. Dehmer, J. Phys. C **7**, L278 (1974).

[19]S. T. Pantelides, Phys. Rev. B **11**, 2391 (1975).

[20]S. T. Pantelides, Solid State Commun. **16**, 95 (1975).

[21]B. I. Dunlap, P. A. Mills, and D. E. Ramaker, J. Chem. Phys. **75**, 300 (1981).

[22]V. E. Henrich, G. Dresselhaus, and H. J. Zeiger, Phys. Rev. Lett. **36**, 158 (1976).

[23]F. P. Netzer, J. A. D. Matthew, and E. Bertel, in *Advances in Spectroscopy: Spectroscopy of Surfaces,* edited by R. E. Hester and R. J. H. Clark (Wiley, Chichester, 1988).

[24]C. E. Moore, *Atomic Energy Levels,* U.S. National Bureau of Standards Circular No. 467 (U.S. GPO, Washington D.C., 1949).

[25]T. Blechschmidt, R. Haensel, E. E. Koch, U. Nielsen, and M. Skibowski, Phys. Status Solidi B **44**, 787 (1971).

[26]N. V. Smith and D. P. Woodruff, Prog. Surf. Sci. **21**, 295 (1986).

[27]F. P. Netzer, J. U. Mack, E. Bertel, and J. A. D. Matthew, Surf. Sci. **160**, L509 (1985).

[28]E. W. Plummer, C. T. Chen, W. K. Ford, W. Eberhard, R. P. Messmer, and H.-J. Freund, Surf. Sci. **158**, 58 (1985).